IMPACT OF MAGNETIC ENVIRONMENT ON THE GENERATION OF HIGH-ENERGY NEUTRONS AT THE SUN

L. G. KOCHAROV and J. TORSTI

Space Research Laboratory, Department of Physics, SF-20014 Turku University, Finland

F. TANG and H. ZIRIN

Big Bear Solar Observatory, Caltech, Pasadena CA 91125, U.S.A.

G. A. KOVALTSOV and I. G. USOSKIN

Ioffe Physical-Technical Institute, St. Petersburg 194021, Russia

Abstract. This paper demonstrates the important interplanetary manifestation of strongly tilted magnetic fields at the flare site. We start with analysis of Big Bear Solar Observatory (BBSO) observations of magnetic structures at sites of two flares responsible for > 100 MeV neutron events. Based on these observations, a model of neutron production is considered. This model takes into account the observed large tilt of magnetic field lines at footpoints of flare magnetic loops. Results of the new calculations are compared with both previous calculations and observations. The tilt of magnetic field lines at the flare site is proved to be the most important parameter limiting anisotropy of high-energy secondary emission in solar flares.

1. Introduction

The acceleration of particles is an important part of the solar flare problem. A number of acceleration models have been proposed (e.g., Anastasiadis and Vlahos, 1994, and references therein). All the acceleration models face a common problem: they have no reliable observational spectra of interacting ions to be used as a basic criterion for the model. One should use γ-ray and neutron emissions to deduce spectra of high-energy ions interacting at the Sun (for a review see Mandzhavidze and Ramaty, 1993). For instance, the 2.22 MeV to the 4–7 MeV γ-ray line fluence ratio is a sensitive function of the ion spectrum slope at $\sim$30 MeV, but it gives almost no information about proton spectrum above 100 MeV. For this reason, both the power law and the Bessel function type spectra of accelerated ions are used to fit the fluence ratios observed (e.g., Ramaty *et al.*, 1993). Furthermore, it is known that the 2.22 MeV to the 4–7 MeV fluence ratio may also depend on the angular distribution of interacting ions (Hua and Lingenfelter, 1987). To deduce the spectrum of interacting ions at higher energies, $>$100 MeV, one has to study $>$50 MeV neutrons and π^0-decay γ-rays. When studying these emissions, the angular distribution of interacting particles turns out to be even more important because of possible anisotropy of any high-energy emission produced. This implies that ion spectra cannot be accurately deduced from γ-ray and neutron data without a study of the angular distribution of interacting particles.

In solar cycle 22, observations of high-energy γ-ray and neutron flares suggest more isotropic production of high-energy neutral emissions than was expected earlier (Mandzhavidze and Ramaty, 1993, Vilmer *et al.*, 1993). One possible explanation of these observations is that the high-energy emissions are produced in complex magnetic structures with varying configurations from flare to flare (Chupp *et al.*, 1993, Trottet *et al.*, 1993). However, this hypothesis has not been quantitatively verified. In this paper we study the magnetic environment at sites of two flares responsible for high-energy neutron and γ-ray events detected at the Earth's orbit. Then we calculate the transport and interaction of accelerated ions, taking into account the tilted magnetic fields observed.

2. Observations

Two well-known neutron-emitting flares (e.g., Kocharov *et al.*, 1994, 1995) were observed at Big Bear Solar Observatory on 24 May 1990 and 22 March 1991. In particular, high-resolution observations in the helium D3 line (5876 Å) are available for these flares. The D3 images were taken at a 3 per min rate with a spatial resolution of about 1 arc sec. Vector magnetograms (VMGs) with a spatial resolution of about 2 arc sec are available for the 22 March 1991 flare only.

It is known that accelerated particle streams and thermal conduction may result in D3 brightenings in flares (Zirin, 1988). To examine the connection between D3 brightening and the precipitation of accelerated particles, we compared D3 light curves obtained at BBSO and the intensity-time profiles of the hard X-ray emission detected on board the GRANAT satellite (Pelaez *et al.*, 1992, Terekhov *et al.*, 1996). To obtain the D3 light curve, the digitized images of the D3 filtergrams were obtained first. A small portion of each image that includes only the flare region is selected such that the background is minimal and the same in all the frames. Then a flare threshold above the actual background is determined. The light curve is the number of pixels above this threshold at different times during the flare. The result is shown in Figure 1. Shown in the same figure is the time profile of $\sim$100 keV hard X-ray emission. Coincidence of D3 and hard X-ray brightenings is seen clearly at the onset of both flares. This supports the idea that the D3 emission was initially caused by penetration of accelerated particles deep into the solar atmosphere. For this reason, we use D3 images to ascertain the site where accelerated particles hit the solar chromosphere.

Figure 2 shows two D3 frames obtained in the beginning and near the maximum of the 1990 May 24 flare (N33 W78). The flare started with two chains of brightenings which later developed into two bright ribbons situated in magnetic field regions of opposite polarity. Hence, one can regard these chains as footpoints of the small arcade where accelerated particles precipitated. Late in the flare, at about 21:29 UT, as the temperature cooled, one of the loops was seen in Hα + 0.6 Å. Seen in the projection plane, the loop legs were tilted at about $70°$ and $45°$ with
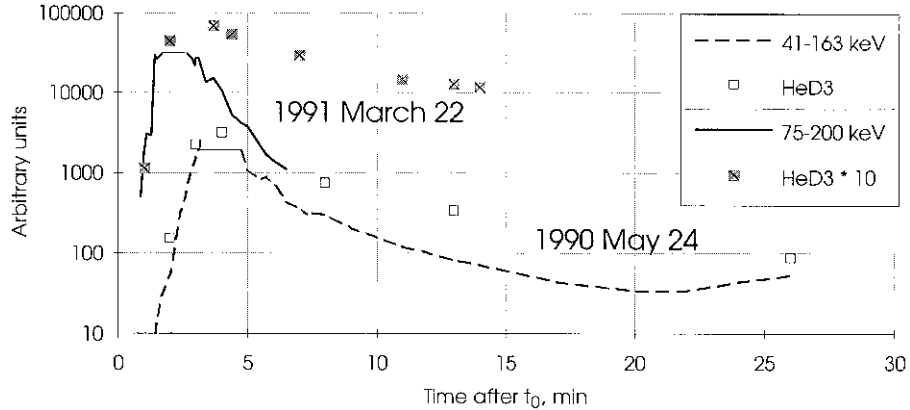
Figure 1. Hard X-ray count rates and HeD3 bright areas for two flares responsible for neutron/γ-ray events. t_0 is 22:42 UT on 22 March 1991 and 20:45 UT on 24 May 1990.

respect to the solar horizon. Note that in the earlier study (Kocharov *et al.*, 1994) such relatively small loops of $\sim 2 \times 10^9$ cm length were considered to be the place where the first component of the high-energy ions was confined. And some much larger loop was suggested for more prolonged confinement of the second component of accelerated ions.

The D3 image near the maximum of the 1991 March 22 flare (S26 E28) is shown in Figure 3. Basically four sources of emission, A_1, A_2, B_1, B_2, were seen at opposite sides of the neutral line of the magnetic field, which is also indicated in the figure. Later in the flare, at about 22:53 UT, several magnetic loops connecting $A_1 B_1$ and $A_2 B_2$ were seen in absorption. From the fact that they were observed in absorption, we may deduce that their density was below 5×10^{12} cm^{-3} (see Zirin, 1988). The distance between the footpoints was $(1.5 - 6) \times 10^9$ cm. The vector magnetogram from BSSO was used to calculate the angle between the line of sight and the solar magnetic field (see Figure 2 by Kocharov *et al.*, 1995, where east is to the right). The view angle is found to be predominantly about $45°$ in sources situated to the west and about $90°$ to the east of the neutral line. Taking into account the position of the flare on the solar disk, one can deduce that the dominant tilt of the magnetic field lines with respect to the solar surface was about $80°$ and $35°$ in the west and east sources, respectively. Thus we conclude that, in both flares, magnetic field lines were essentially tilted at one or both footpoints of the loops where hard emissions are generated.

3. Model and Results of Calculations

Let us consider the transport and interaction of accelerated particles in a magnetic loop with field lines tilted at one or both footpoints. Neutrons with energies >100 MeV are mostly produced in (p,p), (p,He) and (He,He) interactions

90-5-24
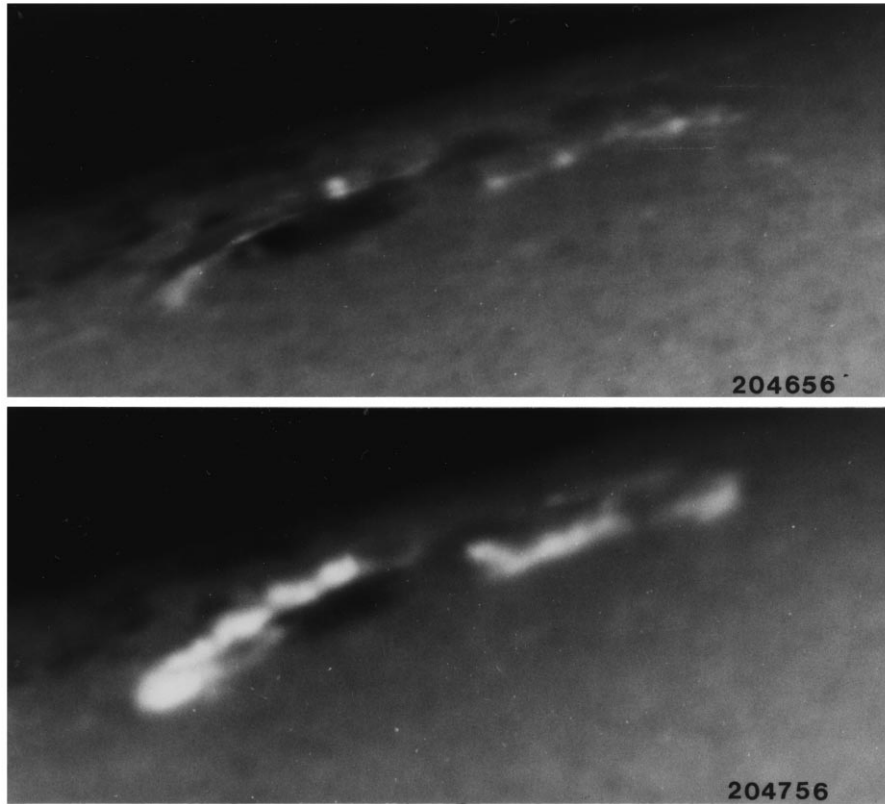
Figure 2. The 1990 May 24 flare shown in D3. North is to the left, west is on top.

and are emitted preferentially in the direction of the incident particle. Note that bremsstrahlung γ-rays produced by ultra-relativistic electrons are emitted also preferentially along the direction of motion of the electron, but the cross-section is more anisotropic. For these reasons, the impact of the magnetic environment on the production of high-energy neutral emissions may be clearly shown when analyzing the distribution of primary particles at the instant of interaction. Thus, as a result of Monte Carlo simulations, we obtain the angular distribution of primary protons at the instant the secondary neutron is produced, $F(\varphi, \vartheta)$. The polar angles φ and ϑ are defined in the frame of the loop (Figure 4(b)). The function $F(\varphi, \vartheta)$ is normalized to unity for an isotropic distribution of the interacting particles. One can introduce certain simplifications when the only aim is to study the impact of the tilted field lines on the angular distribution of the high-energy secondary emission. In particular, the model does not attempt to consider the temporal evolution of the energy spectrum of accelerated particles. Accelerated particles are proposed to be injected at the top of the loop and the initial energy of all primary particles is E_0,
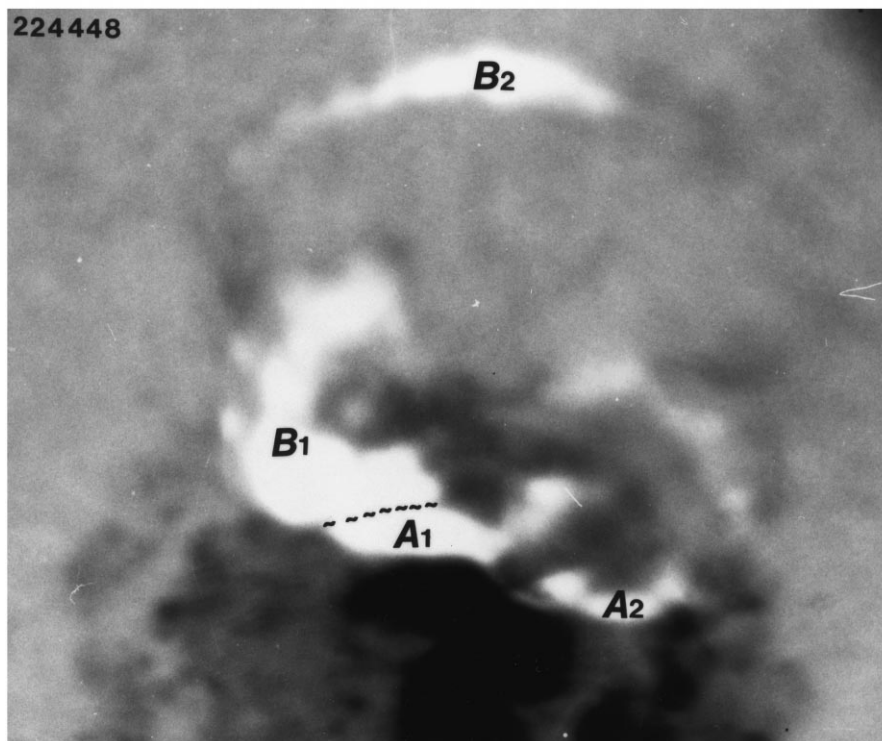
Figure 3. The 22 March 1991 flare shown in D3. The black dashed line indicates the magnetic neutral line. North is to the right, and east is on top.

which is the 'effective' energy for the emission generation. For production of neutrons detected by ground based neutron monitors, $E_0 = 600$ MeV. In the coronal part of the loop (of height R), the magnetic field strength as well as number density are considered to be constant, B_c and n_c, respectively. In the chromosphere, the magnetic field increases downward with depth, $Z \leq 0$: $B = B_c(1 - Z/h_m)$, while the magnetic field is constant in the photosphere: $B = B_{ph}$. The density increases downward with depth: $n = n_0 \exp(-Z/h_A)$ (at $Z = 0$, there is an abrupt density increase from n_c to $n_0 \gg n_c$). The mirror ratio, $\rho = B_{ph}/B_c$, is considered to be the same for both footpoints, but the tilt of magnetic field lines, α, may be different (Figure 4(b)). We trace the propagation of accelerated ions inside the loop, taking into account the pitch-angle scattering on small-scale magnetic inhomogeneities (MHD turbulence), energy losses and nuclear interactions (similar to Guglenko *et al.*, 1990). The mean free path describing the pitch-angle scattering, λ, is considered to be less than the loop length.

In Figure 4(a) is shown the angular distribution of interacting protons in the loop plane ($\varphi = 180°$) for two cases: (1) both loop legs are vertical, (2) one
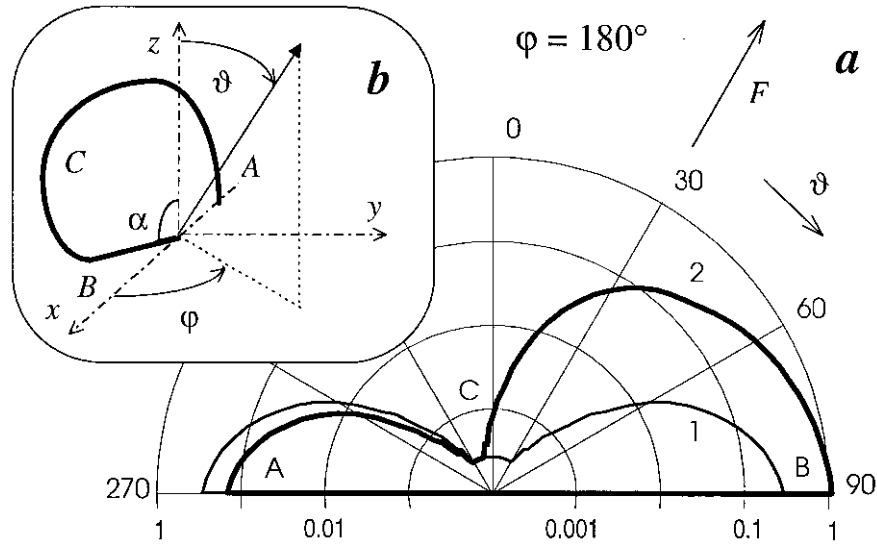
Figure 4. (a) Angular distribution of protons at the instant of neutron production shown in the loop plane for two cases: (1) both loop legs are vertical, (2) one leg is tilted by $\alpha = 45°$. (b) The loop model employed. Parameters of the loop: $R = 2 \times 10^9$ cm, $n_c = 10^{11}$cm^{-3}, $h_m/h_A = 2.5$, $\rho = 5$, $n_0 = 10^{13}$cm^{-3}, $\lambda/(\pi R) = 0.1$.

leg is tilted by $45°$ as shown in Figure 4(b). The first case was adopted in many previous calculations (for a review see Ramaty and Mandzhavidze, 1994). Taking into account the logarithmic scale applied, the impact of the magnetic tilt is seen to be very strong. In Figure 5, we show the pattern of two-dimensional distribution of interacting protons for the case where both loop legs are tilted by $45°$.

4. Discussion and Conclusions

Results of Monte Carlo simulations are in agreement with the approximated analytical consideration by Kocharov and Kovaltsov (1995). It was concluded that, in the direction normal to the magnetic field at the footpoint, the distribution of interacting particles, $F_\perp$, is rather weakly dependent on model parameters, provided that the magnetic mirror is thick enough to strongly decelerate trapped particles with smallest pitch angles and $\rho h_m/h_A \gg 1$. In this case, the value of the distribution function may be estimated as

$$F_\perp \approx 0.5\Big(\ln((\Lambda \cos\alpha)/(n_0 h_A)) - 0.5\ln(h_m/h_A) + h_m/h_A - 2\Big)^{-1/2}, \quad (1)$$

where the contribution of only one magnetic mirror is taken into account, Λ is the path length describing both Coulomb and nuclear losses. The typical value of $F_\perp$ is 0.15. These particles interact while mirroring, and their emission dominates in
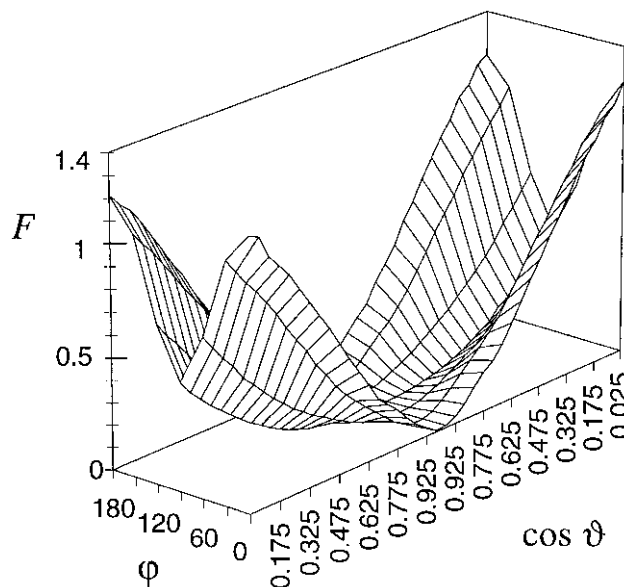
Figure 5. The distribution of protons at the instant of neutron production. Both loop legs are tilted by 45° in the loop plane (for another parameters see Figure 4).

the direction $\varphi = 180°$, $\vartheta = 270°$ (marked with A in Figure 4(a)). On the other hand, in the case of the tilted magnetic field, emission in the direction $\varphi = 180°$, $\vartheta = 90°$ (marked B in Figure 4(a)) is mainly produced by non-mirrored particles. The intensity of this emission may exceed that produced in the isotropic case. Provided that the loop legs are not sufficiently tilted, the emission in the upward direction (marked C in Figure 4(a)) is predominantly generated by particles in the coronal portion of the loop (C in Figure 4(b)). For this emission, the distribution of interacting particles is isotropic and depends on trapping time, τ, and density at the top of the loop: $F_{\|} \approx (n_c v \tau)/\Lambda$, where v is particle velocity.

It is seen that the tilt of the magnetic field at loop footpoints is the most important parameter affecting the observed intensity of > 100 MeV neutrons and other high-energy secondary emissions. In the case of the tilted field, neutron emission of the same order of magnitude may be observed from flares with heliocentric angles $\approx 35°$ and $\approx 80°$ (e.g., $\vartheta \approx 35°$ in Figure 4(a), and $\vartheta \approx 80°$, $\varphi = 90°$ in Figure 5, respectively). Recently Kocharov *et al.* (1995) compared high-energy neutron emissions from the 24 May 1991 and 22 March 1991 flares and concluded that the relative brightening of the 24 May 1990 flare due to the difference in flare heliocentric angles did not exceed a factor 3. This result may be easily explained because, in the case of the 22 March 1991 flare, the magnetic field at the east footpoints was strongly tilted, as indicated by BBSO magnetograms. Our calculations reveal strong sensitivity to the magnetic tilt angles. To deduce these angles, high-resolution VMGs are required.

Thus we conclude the following: (1) the tilt of magnetic field lines at footpoints of flare loops is a key parameter for theoretical calculations of the anisotropy of high-energy neutron and γ-ray emissions. This parameter was not taken into account in previous calculations. (2) The large magnetic tilt angles actually observed imply much more isotropic emission than that expected in earlier studies. (3) High-resolution magnetograms and stereoscopic observations of γ-ray and neutron emissions are desirable for a more accurate determination of parameters of accelerated ions at the Sun.

Acknowledgements

References

Anastasiadis, A. and Vlahos, L.: 1994, *Astrophys. J.* **428**, 819.

Chupp, E. L., Trottet, G., Marschhaser, H., Pick, M., Soru-Escaut, I., Rieger, E., and Dunphy, P. P.: 1993, *Astron. Astrophys.* **275**, 602.

Gueglenko, V. G., Kocharov, G. E., Kovaltsov, G. A., Kocharov, L. G., and Mandzhavidze, N. Z.: 1990, *Solar Phys.* **125**, 91.

Hua, X.-M. and Lingenfelter, R. E.: 1987, *Solar Phys.* **107**, 351.

Kocharov, L. G. and Kovaltsov, G. A.: 1995, *Proc. 24th Int. Cosmic Ray Conf.* **4**, 82.

Kocharov, L. G., Lee, J. W., Zirin, H., Kovaltsov, G. A, Usoskin, I. G., Pyle, K. R., Shea, M. A., and Smart, D. F.: 1994, *Solar Phys.* **155**, 149.

Kocharov, L. G., Lee, J. W., Wang, H., Zirin, H., Kovaltsov, G. A, and Usoskin, I. G.: 1995, *Solar Phys.* **158**, 95.

Mandzhavidze, N. and Ramaty, R.: 1993, *Nuclear Phys.* **B33**, 141.

Pelaez, F., Mandrou, P., Niel, M., Mena, B., Vilmer, N., Trottet, G., Lebrun, F., Paul, J., Terekhov, O., Sunyaev, R., Churazov, E., Gilfanov, M., Denisov, D., Kuznetsov, A., Dyachkov, A., and Khavenson, N.: 1992, *Solar Phys.* **140**, 121.

Ramaty, R. and Mandzhavidze, N.: 1994, in J. M. Ryan and W. T. Vestrand (eds.), *High-Energy Solar Phenomena, AIP Conf. Proc.*, **294**, 26.

Ramaty, R., Mandzhavidze, N., Kozlovsky, B., and Skibo, J. G.: 1993, *Adv. Space. Res.* **13** (9), 275.

Terekhov, O., Sunyaev, R., Tkachenko, A., Denisenko, D., Kuznetsov, A., Barat, C., Dezalay, J.-P., and Talon, R.: 1996, *Pis'ma v Astron. Zh.* **22** (3), 163.

Trottet, G., Vilmer, N., Barat, C., Dezalay, J.P., Talon, R., Sunyaev, R., Terekhov, O., and Kuznetsov, A.: 1993, *Adv. Space. Res.* **13** (9), 285.

Vilmer, N., Trottet, G., Barat, C., Dezalay, J.P., Talon, R., Sunyaev, R., Terekhov, O., and Kuznetsov, A.: 1993, *Lecture Notes in Physics, Proc. 7th Europ. Meeting on Solar Physics, Catania*, 3.

Zirin, H.: 1988, *Astrophysics of the Sun*, Cambridge University Press, Cambridge.